ENGINEERING TRANSACTIONS • *Engng. Trans.* • **51**, 1, 87–101, 2003
Polish Academy of Sciences • Institute of Fundamental Technological Research
10.24423/engtrans.502.2003

FREQUENCY REDUCTION IN ELASTIC BEAMS DUE TO A STABLE CRACK: NUMERICAL RESULTS COMPARED WITH MEASURED TEST DATA

U. Andreaus, P. Casini, and F. Vestroni

**Dipartimento di Ingegneria Strutturale e Geotecnica,
Università degli Studi di Roma "La Sapienza",
18 Via Eudossiana, 00184 Roma**
e-mail: paul.casini@uniroma1.it

The presence of a crack could not only cause a local variation in the stiffness, but it could affect the mechanical behaviour of the entire structure to a considerable extent. The frequencies of natural vibrations, amplitudes of forced vibrations and areas of dynamic stability change due to the existence of such cracks. The vibration characteristics of cracked structures can be useful for non-destructive testing. In particular, the natural frequencies and mode shapes of cracked beams can provide insight into the extent of damage. The beam has been schematized as a 2-D continuous medium and discretized by means of quadrilateral finite elements. The lowest three natural frequencies (and the associated mode shapes) of the cracked cantilever beam, were obtained via both the modal and spectral analyses, and were compared with experimental data from literature in order to assess the reliability of different models of crack state, namely open crack and contact crack. Both the experimental and numerical results reveal the significant influence of the opening and closing conditions of the crack on the frequency reduction; namely this reduction decreases as more realistic contact phenomena are considered at crack interfaces.

1. Introduction

Although machines and structures are carefully designed for fatigue loading, possess high levels of safety, are constructed with high quality materials, and thoroughly inspected prior to service as well as periodically during their operating lives, still there are instances of cracks or damage escaping inspections. Therefore, the development of structural integrity monitoring techniques have received increasing attention in recent years [6]. Among these monitoring techniques, it is believed that the monitoring of the global dynamics of a structure offers favourable alternative if the on-line (in service) damage detection is

necessary. In fact, non-destructive testing can be performed without actually dismantling the structure. In order to identify structural damage for vibration monitoring, the study of the changes of the structural dynamic behaviour due to cracks is required for developing the detection criterion [19, 23].

Cracks found in structural elements have various causes. They may be fatigue cracks that take place under service conditions as a result of the limited fatigue strength. They may also be due to mechanical defects. Another group involves cracks which are inside the material: they are created as a result of manufacturing processes. For an appreciation of the physical aspects of the problem the reader is referred to the influential paper by GUDMUNDSON [9].

With the ever increasing sophistication of available equipment, more effective models had to be built to better interpret the experimental results. As far as monodimensional continuous models are concerned, two approaches are considered, namely continuous and local flexibility. In the continuous flexibility scheme, differential equation and the boundary conditions are derived for the cracked beam via variational principles [5, 19, 3]. In particular, the modification of the stress field induced by the crack is incorporated through a local empirical function which assumes an exponential decay with the distance from the crack, and includes parameters that had to be evaluated by experiments or using the displacement field in the vicinity of the crack found with fracture mechanics methods (stress intensity factors). In the local flexibility models [9, 14, 17, 1, 4, 21], the main idea in modelling the crack is to introduce a local compliance matrix, connecting longitudinal, bending and shear forces and displacements near the crack tip; the elements of the local flexibility matrix describe the reduced stiffness due to the crack by means of the stress intensity factors [22].

Alternatively the cracked beam can be discretized via the Finite Element Method by using both 1-D [8, 15, 18] and 2-D elements [10, 24, 12].

In addition, the nonlinear behaviour of a beam with a closing crack vibrating in its lowest modes of vibration can be simulated through multi-degree-of-freedom models with bilinear stiffnesses [10, 7, 1, 16].

In the development of some theoretical models, it has been assumed that the crack remains open [9, 5, 14, 8, 17, 3]. In order to validate the open crack models, a static preload has been introduced in experimental tests which keeps the crack open [3, 17, 11, 16].

While the beam is vibrating, the state of the crack section varies from tension to compression, i.e. the crack opens and closes with time. This results in a modification of the crack section stiffness, the extremal values being the stiffness of the open crack and that of the intact beam. Thus, the nonlinear behaviour of the closing crack introduces the characteristics of the nonlinear systems. However, for many practical applications, the system can be considered bi-linear,

and the fatigue crack can be introduced in the form of the so-called "breathing crack" model which opens when the normal strain near the crack tip is positive, otherwise it closes [24, 10, 15, 19, 1, 18, 16]. Crack closure during half of the vibratory cycle causes a smaller drop in the eigenfrequencies. Thus, relying on the drop in the natural frequencies only and using the open crack model could lead to underestimating the severity of the crack [4].

The crack closure effect was experimentally investigated for an edge-cracked beam with a fatigue crack [9, 12] and it was found that the eigenfrequencies decreased, as functions of crack length, at a much slower rate than in the case of an open crack. Thus, the interfaces forces are needed for the modelling of interface normal contact and dry friction [1, 12].

The recent literature suggests that the nonlinear component of motion of a cracked beam must be accorded increasing importance where accuracy is important in a system model. Few response analyses of cracked structures have taken into account the effect of alternation of the crack opening and closure. Therefore, the aim of the present paper is twofold: (i) to investigate the free response of the cracked beam after an impulsive loading via spectral analysis, and (ii) to compare the previous numerical results with measured test data known from literature. A beam is considered as a 2-D solid body and the finite element method is used to discretize both the continuum and the crack interfaces. Models of open and breathing cracks are compared in terms of frequency reduction.

2. System model

2.1. Generalities

Figure 1 shows a cantilever beam with a single-side edge-crack; the straight beam of length L and rectangular uniform cross-section is clamped at the left end and free at the right end. The crack is located at the upper edge of the beam at a distance z from the fixed end and $\zeta = z/L$ is the dimensionless crack position; the severity $s = a/h$ of the crack is expressed in terms of the ratio between its depth, a, and the height of the beam, h. Linear isotropic stress-strain material properties are assumed.

A cracked cantilever beam of length 300 mm and cross-section 20×20 mm^2, with *Young*'s modulus $E = 2.068 \times 10^5$ Mpa, *Poisson's* ratio $\nu = 0.3$, and mass density $\rho = 7850$ kg/m^3, Fig. 1, was tested and studied by Rizos *et al.* [17]. The vibration frequencies and mode shapes of the beam containing an edge-crack of various sizes at different positions along the beam were obtained by Kam & Lee [11] from either experiments [17] or finite element analyses of the cracked beam when experimental data were not available. In the case of the finite element analyses of the cracked beam, the stiffness matrix of the cracked

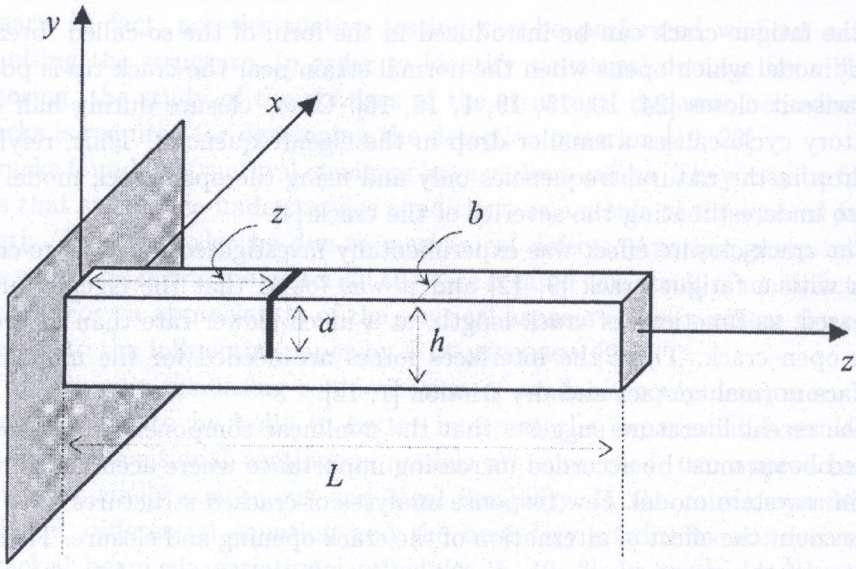

FIG. 1. Cantilever beam with a transverse single-side edge-crack.

element proposed by QIAN *et al.* [15] was used to generate the required data for crack identification.

The mechanical behaviour of an opening crack is different from that of a closing crack. To analyze these behaviours in fracture mechanics when general time-varying loads are applied is a very complex problem; in fact the stress-strain field at the crack tip, the form of the crack interface and the level of the crack's opening and closing are all required [15]. Thus, the equations of motion are nonlinear and nonsmooth, and, definitively, there is no exact solution of these equations. Consequently, a numerical method [9, 24, 12] must be adopted. Herein, the plane-stress elastodynamic response of an edge cracked panel (2-D body, i.e. a strip) is studied; both modal and spectral analyses have been performed using a proprietary finite element package (ADINA 7.4). The finite element mesh consisted of 2-D solid plane stress 8-node isoparametric elements. A consistent mass matrix is used with implicit time integration, provided that the Newmark method and full Newton iteration are used. Two-dimensional contact surfaces are specified to model the planar contact behaviour between 2-D solid elements at the crack interfaces, Fig. 2.

2.2. Contact modelling

Contact surfaces are defined as surfaces that are initially in contact or are anticipated to come into contact during the response solution. Two-dimensional contact surfaces are formed of a series of linear contact segments and each seg-

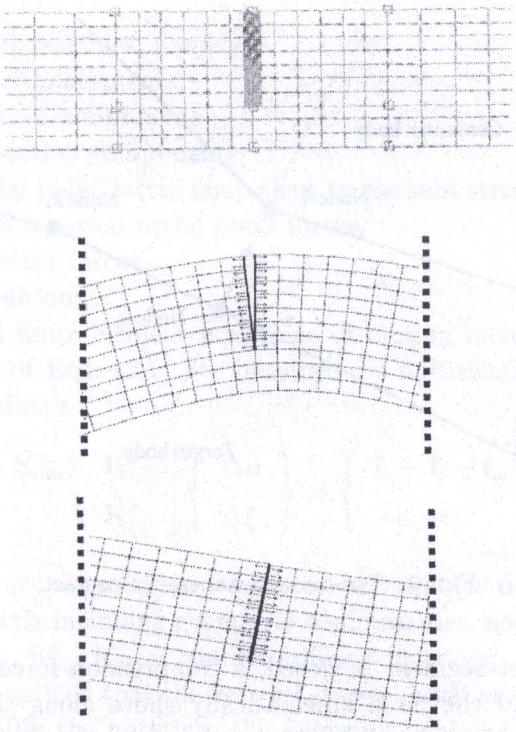

FIG. 2. Mesh zoom of the crack zone.

ment is bounded by two nodes, Fig. 3. Two contact surfaces that are initially in contact or that are expected to come into contact during the response solution, form a contact pair. An important distinction should be made in a contact pair between the contactor surface and the target surface, inasmuch in the converged solution, the target nodes can overlap the contactor body and not vice-versa; in other words, after satisfaction of the contact condition, the contactor nodes cannot be inside the target body, but the target nodes can be inside or outside the contactor body. A node of the contactor surface can come into contact with a segment of the target surface.

In frictionless contact, the possible states of the contactor nodes and/or segments are: (i) the gap between the contactor node and target segment is open (no-contact); (ii) formerly closed gap has opened; a tensile force acting onto the contactor node is not possible (tension release); (iii) the gap between the contactor node and the target segment is closed; a compression force is acting onto the contactor node and the node kinematically slides along the target segments (sliding).

In frictional contact, (i) the states of "no-contact" and "tension release" are as for the case of frictionless contact. Otherwise (ii) the gap between the contactor

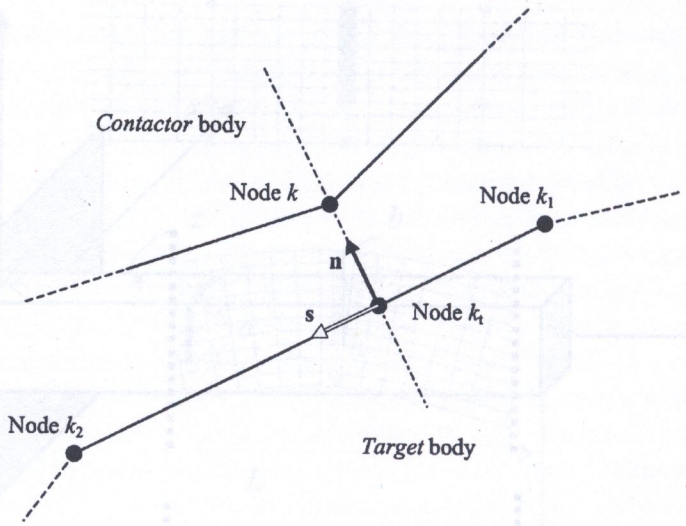

FIG. 3. Two-dimensional case of contact.

node and the target segment is closed, a compression force is acting onto the contactor node, and the node kinematically slides along the target segments with the restrictive force to sliding being equal to the Coulomb friction force (sliding); (iii) as long as the tangential force on the contactor node that initiates sliding is less than the frictional capacity (equal to the normal force times the Coulomb friction coefficient), the contactor node sticks to the target segment (sticking).

The finite element solution of the governing continuum mechanics equations is obtained by using the discretization procedures for the principle of virtual work, and in addition now discretizing the contact conditions also. To exemplify the formulation of the governing finite element equations, let us consider the two-dimensional case of contactor and target bodies shown schematically in Fig. 3, where the target segment corresponding to contactor node k is defined by nodes k_1 and k_2. The target point k_t is the closest point of the target segment $k_1 - k_2$ to the contactor node k. By assembling for *all* contactor nodes the nodal point force vectors, the discretization of the continuum mechanics equations corresponding to the conditions at time $t+\Delta t$ gives [2]

$$\begin{aligned} \mathbf{f}_i(\mathbf{u}) &= \mathbf{f}_e - \mathbf{f}_c(\mathbf{u}, \xi) = \mathbf{0}, \\ \mathbf{c}_c(\mathbf{u}, \xi) &= \mathbf{0}, \end{aligned} \tag{2.1}$$

where

$$\xi^T = \{\lambda^T, \tau^T\},$$

$\mathbf{u}$, λ, τ – solution variables, namely
$\mathbf{u}$ – nodal point displacements,
λ – normal traction components,
τ – tangential traction components,
$\mathbf{f}_i$ – internal nodal point forces equivalent to element stresses,
$\mathbf{f}_e$ – total applied external nodal point forces,
$\mathbf{f}_c$ – updated contact forces,
$\mathbf{c}_c$ – contact conditions.

The incremental finite element equations of motion including contact conditions for solution of Eqs. (2.1) are obtained by linearization about the last calculated state at time t :

$$\begin{bmatrix} (\mathbf{K}+\mathbf{K}^c_{uu}) & \mathbf{K}^c_{u\xi} \\ \mathbf{K}^c_{\xi u} & \mathbf{K}^c_{\xi\xi} \end{bmatrix} \begin{Bmatrix} \Delta\mathbf{u} \\ \Delta\xi \end{Bmatrix} = \begin{Bmatrix} \mathbf{f}_e - \mathbf{f}_i - \mathbf{f}_c \\ -\mathbf{c}_c \end{Bmatrix} \tag{2.2}$$

where: $\Delta\mathbf{u}$ and $\Delta\xi$ = increments in the solution variables $\mathbf{u}$ and ξ, K = usual tangent stiffness matrix including geometric nonlinearities, not including contact conditions, K^c_{uu}, $\mathrm{K}^c_{u\xi}$, $\mathrm{K}^c_{\xi u}$, $\mathrm{K}^c_{\xi\xi}$ = contact stiffness matrices;

It is worth to be noticed that the vector $\mathbf{f}_e$ is evaluated at current time $t+\Delta t$.

In order to simplify the notation, the following relations are understood to refer to any contactor node k. Using the definition of the "gap function" g, that is the (signed) distance from the node k to the node k_t, the conditions for normal contact can be stated as the SIGNORINI'S in displacements conditions [20]

$$g \geq 0, \quad \lambda \geq 0, \quad g\lambda = 0, \tag{2.3}$$

where λ is the normal traction component.

Moreover, Coulomb's law of friction states that [13]

$$\begin{aligned} &h \geq 0, \quad \gamma \geq 0, \quad h\gamma = 0, \\ &\lambda\,(\dot{u} - \gamma\tau) = 0, \\ &h = \mu\lambda - \tau, \end{aligned} \tag{2.4}$$

where:
γ – any nonnegative parameter,
μ – the coefficient of friction between contacting surfaces,
τ – the tangential traction component,
$\dot{u}$ – the tangential velocity component at time t of the node k_t with respect to node k,

Equations (2.3) and (2.4) can be interpreted by considering the following cases:

1. *No contact*: If $g>0$, the inequality in (2.3) implies $\lambda=0$. It follows from definition $(2.4)_3$ and the first inequality in $(2.4)_1$ that $\tau=0$. When there is no contact, all contact tractions must be zero. Equation $(2.4)_b$ is trivially satisfied.

2. *Sticking contact*: If $\lambda>0$ and $h>0$, the equalities in (2.3) and $(2.4)_1$ imply $g=0$ and $\gamma=0$. It follows from Eq. $(2.4)_2$ that $\dot{u}=0$. When there is contact and the contact friction force has norm τ less than the frictional resistance $\mu\lambda$, there is no relative motion.

3. *Sliding contact*: If $\lambda>0$ and $h=0$, the equality in (2.3) implies $g=0$ and definition $(2.4)_3$ implies $\tau=\mu\lambda$. It follows from Eq. $(2.4)_2$ that $\dot{u}=\gamma\tau$. When there is contact and the contact friction force has norm τ equal to the frictional resistance $\mu\lambda$, the motion of the target body relative to the contactor body must be in the tangential direction $\mathbf{s}$.

Thus, the components of the vector $\mathbf{c}_c$ which refer to the node k can be written as

$$\begin{aligned} c_{cw} &= w(g,\lambda)\,, \\ c_{cv} &= v(\dot{u},\tau,\mu\lambda) \end{aligned} \tag{2.5}$$

and the following constraint functions can be used:

$$\begin{aligned} w(g,\lambda) &= \frac{g+\lambda}{2} - \sqrt{\left(\frac{g-\lambda}{2}\right)^2 + \varepsilon_N}, \\ v(\dot{u},\tau,\mu\lambda) &= \mu\lambda - \frac{2}{\pi} arctg\left(\frac{\dot{u}}{\varepsilon_T}\right), \end{aligned} \tag{2.6}$$

where ε_N is very small but larger than zero and ε_T is a small parameter which can provide some regularity to the Coulomb friction law.

3. Modal Analysis

The lowest three natural frequencies of the intact beam ($\mathbf{K}^c_{uu} = \mathbf{K}^c_{u\xi} = \mathbf{K}^c_{\xi u} = \mathbf{K}^c_{\xi\xi} = 0$, Eq. (2.2)) have been evaluated by performing the modal analysis of the 2-D finite element model described in Sect. 2: 183.4 Hz, 1126.7 Hz, 3060.8 Hz; the associated mode shapes are depicted in Fig. 4a, where the 1st, 2nd, and 3rd rows refer to the lowest three mode shapes respectively. The lowest three natural frequencies of the cracked beam were determined via modal analysis under the assumption of open crack $\left(\mathbf{K}^c_{u\xi} = 0, \mathbf{K}^c_{\xi\xi} = 0\right)$ and compared with the results of experimental tests in order to assess the reliability of different models of crack state, namely open crack and contact crack. Numerical and experimental results have been normalised with respect to the corresponding eigenfrequencies of the uncracked beam. The relevant mode shapes obtained via the 2-D finite element model are depicted in Fig. 4b.

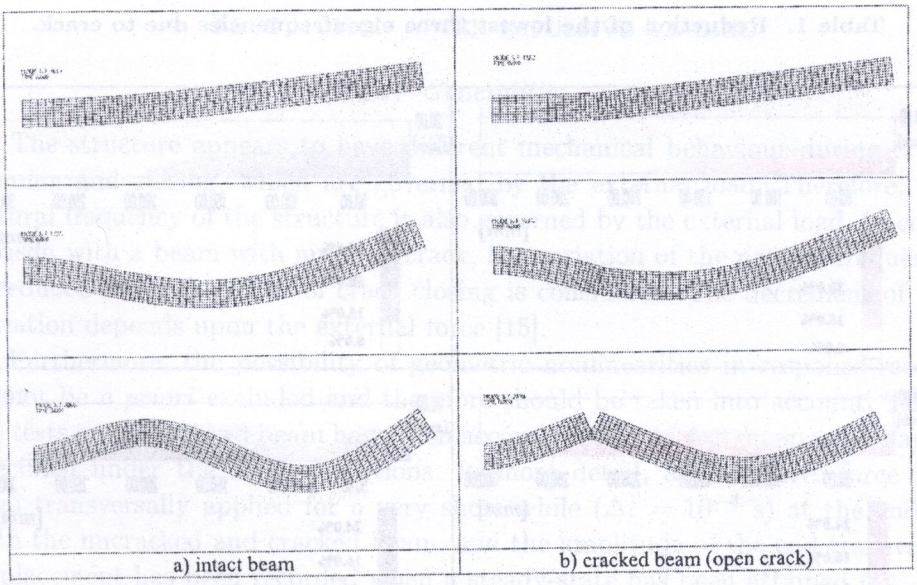

FIG. 4. Mode shapes.

Filled contour maps of Table 1 that fill the area between contour levels, simultaneously illustrate the combined influence of crack position and severity on the lowest three natural frequencies of the cracked beam. Columns (a) and (b) refer to experimental data and open crack models respectively, and the 1^{st}, 2^{nd}, and 3^{rd} rows refer to the lowest three natural frequencies respectively. The two dimensions of each rectangular domain are the length of the beam and the largest crack depth ($a = 0.75$h); more precisely, the co-ordinate axes respectively coincide with the z- and y-axes of the beam, Fig. 1. Fill attributes are assigned so that there is a gradation change of colour from the minimum to maximum contours. Moreover, a colour scale shows the fill assigned to each colour on a filled contour map; a sample of the fill attributes assigned to each level and the numerical value for each level are displayed. The numerical values measure in percentage the difference between the reduced frequency of the cracked beam and the frequency of the uncracked beam, normalised with respect to this latter value. For given position and severity of the crack, the frequency reduction can be estimated by visual means.

The results from experimental tests [11], reported in column a), refer to a crack maintained open by static preloading. A good agreement can be observed between the results obtained via both the physical (column a) and numerical (column b) experimentation.

The influence of the crack on the frequency reduction attains its maxima when the crack is located at the peak/trough positions of the strain mode shapes,

Table 1. Reduction of the lowest three eigenfrequencies due to crack.

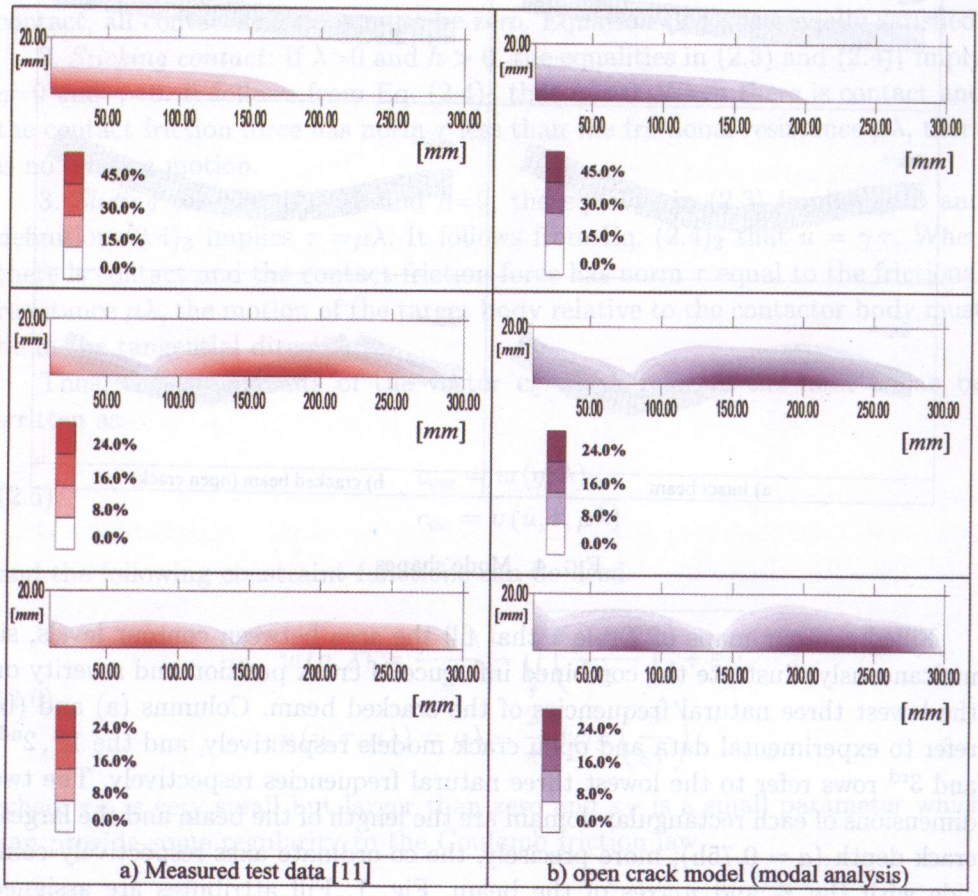

whereas its influence becomes the smallest at mode shape nodes. Furthermore, the influence of the crack, located at the peak/trough positions of each strain mode shape, dramatically drops as soon as one passes from the 1st mode to the higher ones. In more detail, as far as the 1st mode is concerned, when ζ=0.034 and $s = 0.7$ the open and contact crack models give maximum normalised frequency reductions 48.8% *versus* the experimental 53.5%. As far as the 2nd mode is concerned, as expected, two local maxima frequency reductions are encountered for ζ_1=0.034 (open crack: 20.3%; experimental: 21.4%) and ζ_2=0.67 (open crack: 31.1%; experimental: 31.4%). As far as the 3rd mode is concerned, three local maxima frequency reductions are encountered for ζ_1=0.034 (open crack: 13.4%; experimental: 12.1%) and ζ_2=0.267 (open crack: 24.5%; experimental: 17.1%) and ζ_3=0.67 (open crack: 24.6%; experimental: 21.9%).

4. Free motion after impulsive loading

4.1. Generalities

The structure appears to have different mechanical behaviour during crack opening and closing, which are governed by the external load. Therefore, the natural frequency of the structure is also governed by the external load. In comparison with a beam with an open crack, the variation of the natural frequency is reduced when the effect of crack closing is considered. The decrement of the variation depends upon the external force [15].

Furthermore, the possibility of geometric nonlinearities in response record cannot be *a priori* excluded and therefore should be taken into account. Thus, the tests on the cracked beam have been accompanied by a test on an undamaged specimen under the same conditions. In more detail, an impulsive force has been transversally applied for a very short while ($\Delta t = 10^{-4}$ s) at the end of both the uncracked and cracked beam, and the amplitude of the end transverse displacement has been recorded when a steady-state has been attained ($t_{\max} = 3 \times 10^3 \Delta t$). The current numerical tests were conducted to amplitude levels (100 kN) where no geometric nonlinear behaviour was apparent in an undamaged specimen .

4.2. Constant and instantaneous loading

Free vibrations of the cracked beam after impulsive excitation have been numerically analysed under constant and instantaneous loading via the modified Newmark integration method. A point load has been dynamically applied at the cantilever free end and maintained for both the whole duration of the analysis (constant loading, Fig. 5a) and for a very short while (instantaneous loading, Fig. 5b). The constant point force (preloading) has been applied both in the positive and negative verse of the y-axis, in order to separately simulate the different conditions of closeness with full contact and openness of the crack. As it will be observed in the following, since now it can be conjectured that the verse of the instantaneous force (a numerical expedient to simulate the impact hammer experimental technique) is inessential. In all the cases under examination, the frequency content of the displacement time-history of the loaded point node has been determined via spectral analysis.

Filled contour maps of Table 2, similar to those already defined in Sec. 3, show the combined influence of crack position and severity on the lowest three natural frequencies of the cracked beam. Columns (a), (b) and (c) refer to opening and closing preloading, and instantaneous loading respectively, and the $1^{\text{st}}, 2^{\text{nd}}$ and 3^{rd} rows refer to the lowest three natural frequencies respectively.

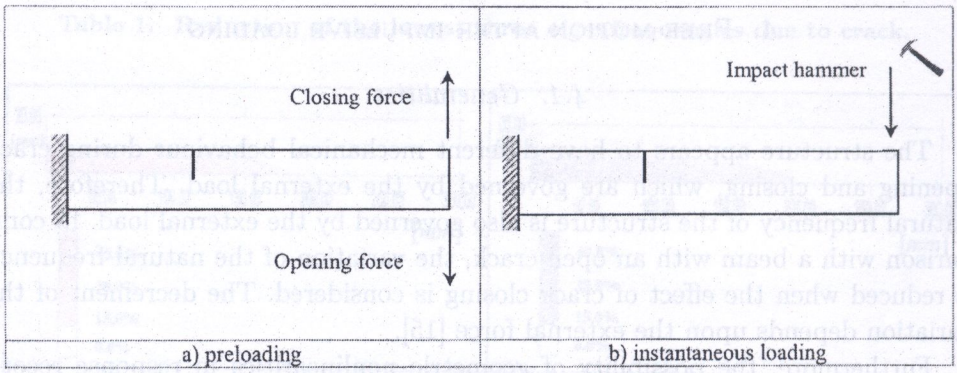

FIG. 5. Impulsive loading.

Table 2. Reduction of the lowest three eigenfrequencies due to crack (spectral analysis).

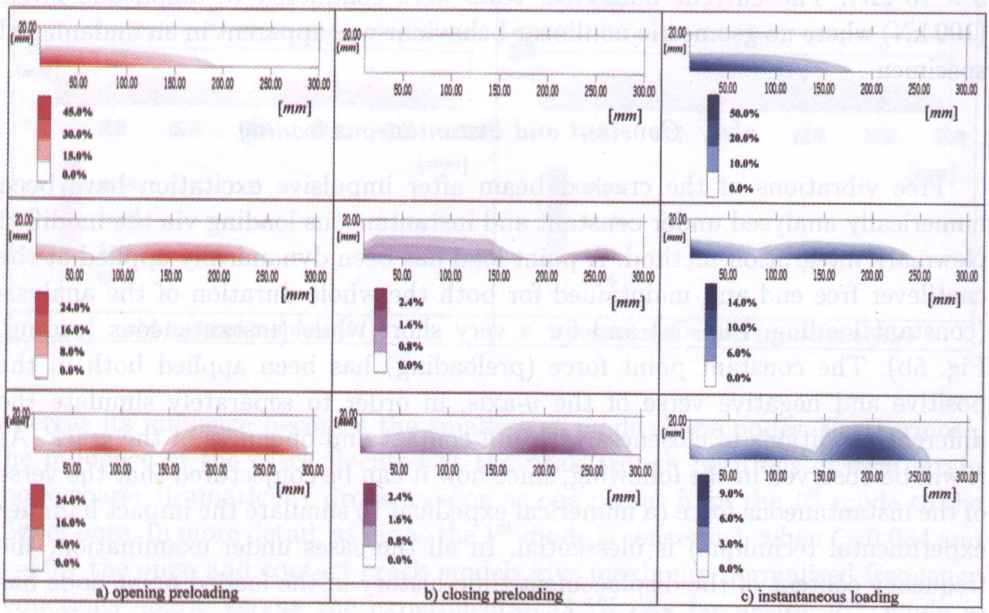

Results illustrated in column (a) of Table 2 refer to beam vibrations when the crack remains almost always open; the comparison between column (a) of Table 2 and the columns in Table 1 shows a good agreement between numerical and experimental results. Results illustrated in column (b) of Table 2 refer to beam vibrations when the crack remains almost always closed; therefore the dynamical behaviour should tend to the condition of uncracked beam. Results

illustrated in column (c) of Table 2 refer to the breathing crack condition. Results reported in column (c) have been numerically demonstrated to be independent of the verse of the instantaneously applied force. As far as the input data are concerned, the integration step is $\Delta t{=}10^{-4}$ s, the duration of the analysis is $t_{\max} = 3{\times}10^{+3}\Delta t$ and the amplitude of both the instantaneous and constant loading is 100 kN.

The 1st row of column b) shows that the crack remains closed due to the preloading; in fact the frequency reduction of the 1st mode is zero everywhere within the domain; this is due to the preloading applied at the peak/trough positions of the 1st mode shape. The same preloading is not efficient as far as the higher modes are concerned; in fact the influence of the crack is not completely annealed, even if the frequency reductions are much smaller than those without preloading (column c).

Column c) shows that the frequency reductions are, as expected, intermediate between open crack and intact beam.

As already observed in the case of modal analysis, the influence of the crack on the frequency reduction attains its maxima when the crack is located at the peak/trough positions of the strain mode shapes, whereas its influence becomes the smallest at mode shape nodes. Furthermore, the influence of the crack, located at the peak/trough positions of each strain mode shape, dramatically drops as soon as one passes from the 1st mode to the higher ones. In more detail, as far as the 1st mode is concerned, when $\zeta{=}0.034$ and $s{=}0.7$, the opening and closing preloading give maximum normalised frequency reductions 47.3%, 0% respectively *versus* instantaneous loading 32.7%. As far as the 2nd mode is concerned, the two local maxima frequency reductions are encountered for $\zeta_1{=}0.034$ (opening preloading: 19.8%; closing preloading: 3.0%; instantaneous loading: 15.4%) and $\zeta_2{=}0.67$ (opening preloading: 31.1%; closing preloading: 1.2%; instantaneous loading: 11.2%). As far as the 3rd mode is concerned, the three local maximal frequency reductions are encountered for $\zeta_1{=}0.034$ (opening preloading: 11.0%; closing preloading: 2.0%; instantaneous loading: 5.1%) and $\zeta_2{=}0.267$ (opening preloading: 23.2%; closing preloading: 1.3% ; instantaneous loading: 6.9%) and $\zeta_3{=}0.67$ (opening preloading: 24.4%; closing preloading: 6.9%; instantaneous loading: 10.5%).

5. Conclusions

On the basis of the numerical results and comparisons worked out in Secs. 3 and 4, the following remarks can be stated, which confirm and extend the conclusions suggested by the literature. Generally speaking, independently of the crack model adopted, the frequency reduction for a single mode increases as the crack gets closer to the peak/trough positions of the mode shape at hand; moreover,

if for each mode we consider the crack located at a peak/trough position, we observe that the influence of the crack decreases from the lowest to the higher modes.

As far as the comparison among the crack models are concerned, the natural frequencies obtained via the breathing crack model lie, as expected, between the natural frequencies of the intact beam and those obtained by the model of the open crack. This is due to the fact that the global stiffness of the system is between the stiffness for the open crack and the intact beam cases, whilst the inertia distribution is unchanged. When the crack closes, there is an increase in the natural frequencies since the system stiffness increases due to the contact effects.

The results from the preceding analysis show that in the absence of sufficient preload, fatigue cracks behave as breathing cracks, resulting in a smaller drop in the natural frequencies than an open-crack model predicts. This is an important factor in applications of the method for crack identification. According to the preloading conditions of the structure under investigation, either the open-crack model or the breathing crack model must be identified. It is evident that using an open-crack model assumption to interpret vibration measurements for a fatigue-breathing crack, will lead to the incorrect conclusion that the crack severity is smaller than what it really is.

References

1. O.N.L. Abraham, J.A. Brandon, *The modelling of the opening and closing of a crack*, ASME J. of Vibration, Acoustics, Stress and Reliability in Design, **117**, 370-377, 1995.

2. K. J. Bathe, *Finite element procedures*, Prentice Hall, Upper Saddle River, New Jersey, 1996.

3. T.G. Chondros and A.D. Dimaronogas, *Vibration of a cracked cantilever beam*, Transaction of the ASME, **120**, 742-746, 1998.

4. T. G. Chondros, A. D. Dimarogonas, J. Yao, *Vibration of a beam with a breathing crack*, J. of Sound and Vibration, 239, **1**, 57-67, 2001.

5. S. Christides, A.D.S. Barr, *One-dimensional theory of cracked Bernoulli-Euler beams*, International Journal of Mechanic Science, **26**, 11/12, 639-648, 1983.

6. I.A. Dimarogonas, *Vibration of cracked structures – A state of the art review*, Eng. Fract. Mech., **55**, 831-857, 1996.

7. M.I. Friswell, J.E.T. Penny, *A simple nonlinear model of a cracked beam*, Proc. of the 10^{th} Int. Modal Analysis Conf., 516-521, California, SanDiego 1992.

8. G. Gounaris, A. Dimarogonas, *A finite element of a cracked prismatic beam for structural analysis*, Computers & Structures, **28**, 3, 309-313, 1988.

9. P. Gudmundson, *The dynamic behaviour of slender structures with cross-sectional cracks*, J. Mech. Phys. Solids, **31**, 4, 329-345, 1983.

10. A. Ibrahim, F. Ismail, and H.R. Martin, *Modelling of the dynamics of a continuous beam including nonlinear fatigue crack*, International Journal of Analytical and Experimental Modal Analysis, **2**, 2, 76-82, 1987.

11. T.Y. Kam, T.Y. Lee, *Detection of cracks in structures using modal test data*, Eng. Fract. Mech., **42**, 2, 381-387, 1992.

12. M. Kisa, J. Brandon, *The effects of closure of cracks on the dynamics of a cracker cantilever beam*, J. of Sound and Vibration, **238**, 1, 1-18, 2000.

13. P. Lötstedt, *Coulomb friction in two-dimensional rigid body systems*, ZAMM, **61**, 605-615, 1981.

14. C.A. Papadopolous, A.D. Dimaronogas, *Coupled logitudinal and bending vibrations of a rotating shaft with an open crack*, Journal of Sound and Vibration, **117**, 1, 81-93, 1987.

15. G.L. Qian, S.N. Gu, J.S. Jiang, *The dynamic behaviour and crack detection of a beam with a crack*, Journal of Sound and Vibration, **138**, 2, 233-243, 1990.

16. A. Rivola, P.R. White, *Bispectral analysis of the bilinear oscillator with application to the detection of fatigue cracks*, Journal of Sound and Vibration, **216**, 5, 889-910, 1998.

17. P.F. Rizos, N. Aspragathos, A.D. Dimarogonas, *Identification of crack location and magnitude in a cantilever beam from the vibration modes*, Journal of Sound and Vibration, **138**, 3, 381-388, 1990.

18. R. Ruotolo, C. Surace, P. Crespo, D. Storer, *Harmonic analysis of the vibrations of a cantilevered beam with a closing crack*, Computers & Structures, **61**, 6, 1057-1074, 1996.

19. M.H.H. Shen, Y.C. Chu, *Vibrations of a beam with a fatigue crack*, Computers & Structures, **45**, 1, 79-93, 1992.

20. A. Signorini, *Lezioni di fisica matematica* (in Italian), E.V. Veschi [Ed.], Rome 1951.

21. J.K. Sinha, M.I. Friswell, S. Edwards, *Simplified models for the location of cracks in beam structures using measured vibration data*, Journal of Sound and Vibration, **251**, 1, 13-38, 2002.

22. H. Tada, P.C. Paris, G.M. Irwin, *The stress analysis of cracks handbook*, Asme Press, New York 2000.

23. F. Vestroni, D. Capecchi, *Damage detection in beam structures based on frequency measurements*, J. Mech. Eng. ASCE, **126**, 7, 761-768, 2000.

24. B. Zastrau, *Vibrations of cracked structures*, Arch. Mech., **37**, 731-743, 1985.

Received May 17, 2002.